

# Numerical and Experimental Analysis of Porosity Effect on the Performance of a Small-scale Thermochemical Reactor

Swaraj Kumar B<sup>1</sup>, Mahesh P V<sup>2</sup>, Sajan Jerome<sup>3</sup>

<sup>1</sup>Department of ME, LBS College of Engineering

<sup>2</sup>Department of ME, LBS College of Engineering

<sup>3</sup>Department of ME, LBS Institute of Technology for Women

\*\*\*

**Abstract** - The process of thermo-chemical energy storage is based on reversible adsorption-desorption reaction, which is endothermic during desorption and exothermic during adsorption. In this work the suitability of Magnesium sulphate ( $MgSO_4$ ) as a thermo-chemical material, is investigated and the parameters affecting the performance of the reactor has been found numerically and one of the most significant parameters is found to be the porosity of the reactor bed. This result is experimentally validated using a small-scale thermochemical reactor setup. An FVM based analysis is performed for the hydration reaction (energy release) of  $MgSO_4$  salt in a packed bed reactor with continuous flow of moist air through the bed. Numerical analysis reveals that the parameters such as porosity of the packed bed, flow rate of moist air across the reactor vessel, particle diameter of the salt, concentration of water vapor at inlet, and heat capacity of the reactor wall, play an important role on the performance of the energy storage system. In experimental analysis the effect of porosity of the reactor bed is analysed and the results shows a good agreement with the numerical prediction.

**Key Words:** Thermal storage, Adsorption Kinetics, thermo-chemical material, Packed bed reactor,  $MgSO_4$

## 1. INTRODUCTION

As the fossil fuel resources are limited and depleting day by day, the gap in energy demand and supply is increasing day by day. This also led to increasing energy cost. Increasing energy consumption also result in considerable impact on the environment, such as climate change and atmospheric pollution. This is a global issue and the problem is likely to aggravate more with time. There is a need to adopt more advanced, efficient and cleaner energy technologies for different applications. Advanced systems for waste energy recovery and energy integration including thermal energy storage (TES) helps to reduce fossil fuel consumption. Thermal energy storage (TES) systems work on the principle of storing the thermal energy in the medium for later utilization. TES technology finds applications in renewable and conventional energy systems to store excess energy during reduced demand situations and supply the stored energy during increased demand state. Thus, TES bridge the gap between energy harvesting and its utilization. Thus, TES is an answer for maintaining a balance between the energy supply and demand for a varying energy consumption pattern. The selection of a TES system for a particular application depends on many factors, including storage duration, economics, supply and utilization temperature requirements, storage capacity, heat losses and available space.

There are two main types of TES systems: (i) sensible, and (ii) latent. Sensible TES systems store energy with changing the temperature of the storage medium, which can be water, brine, rock, soil, etc. Latent TES systems store energy through phase change, e.g., cold storage water/ice and heat storage by melting paraffin wax. Latent TES units are generally smaller than sensible storage units. More compact TES can be achieved based on storages that utilize chemical reactions. Such thermo-chemical storage systems have recently been the subject of increased attention and could be especially beneficial where space is limited

Thermochemical energy storage is one of the promising thermal energy storage methods for solar applications. Its high energy storage density, long term storage capability, ease of transport and high temperature application makes this technology an interesting topic for energy researchers. The research progress in this area are summarized by Juan Wu [1] in his review paper. In this paper he is pointed out that thermochemical energy storage is a promising technology for the future, they also say that more research should have been done in the areas of reaction kinetics, new and advanced storage materials, cycle stability, operating conditions etc.

M. Ghommem et al. [2] has done a numerical analysis of the performance of three salt materials for thermochemical energy storage. In their study they used COMSOL MULTIPHYSICS to solve the problem. Their result shows that Cupric sulphate ( $CuSO_4 \cdot 5H_2O$ ) has the best performance in terms of the efficiency and the gypsum ( $CaSO_4 \cdot 2H_2O$ ) was least efficient. More studies are needed in the area of new composite thermochemical material (TCM) with good heat and mass transfer capabilities, improved design and configuration for reactor and heat exchanger and feasibility of long-term heat storage [3]. The performance of the first experimental work on sorption store for long term storage of solar heat [5] was done at AEE- Institute of sustainable Technologies with silica gel and water vapor as the working pairs. The energy storage density of the TCM was poor in this case. So, the requirement for choosing a TCM for long term application is important in thermochemical energy storage [6]. Another important factor to be considered in selecting a thermochemical material is the solubility of the solid. The less soluble is the solid the higher the probability of achieving the expected reactor yield. There are many variables which will influence the performance of a thermochemical heat storage system [7], they are mass flow rate, ambient temperature, relative humidity and the design of the reactor etc. Another important application of thermochemical energy storage is drying process [8], the drying process is possible during the night hours by using the energy stored during the day time.

Various studies [4, 9-11] had revealed the influence of geometric configuration of the reactor bed, input heat flux, modified Damkohler number, dimensionless thermochemical heat capacity, and the rate of water vapour on the process efficiency. In an experimental work [12], they investigated the hydration/ dehydration cycle of  $\text{Ca}(\text{OH})_2/\text{CaO}$  in two types of reactors. One was a prototype and another was laboratory glassware. Water vapor was added in hydration process. The parameters such as specific heat, reaction rate, enthalpy, mass losses and heat release were monitored for 20 cycles of operation. The result shows no influence of number of cycles in the performance of the system. The chemical reaction did not exhibit the complete reversibility due to the incomplete dehydration of the material. They concluded that the process could not reach the complete dehydrated phase due to the carbonation, future experiments are needed to improve the performance of the reactor.

Different studies were conducted for low temperature thermochemical energy storage technology with different thermochemical materials [13-17], Experiments with magnesium sulphate mono-hydrate and copper sulphate mono- hydrate which are hydrated by a moist air flow show that for both, magnesium and copper sulphate mono hydrate, a higher water vapor pressure is needed for a sufficiently high reaction rate. The dehydration of  $\text{MgCl}_2 \cdot 6\text{H}_2\text{O}$  and subsequent hydration at 12 mbar vapor pressure (corresponding to evaporation at atypical air temperature of 100C) gives a good temperature rise of 200C to the flowing air. This is a promising result for the future use of this material for seasonal domestic heat storage for space heating and tap water heating. The experimental results show that  $\text{MgSO}_4 \cdot 7\text{H}_2\text{O}$  can be dehydrated at temperatures below 150°C, which can be reached by a medium temperature (vacuum tube) collector. Additionally, the material was able to store 2.2 GJ/m<sup>3</sup>, almost nine times more energy can be stored in water as sensible heat. On the other hand, the experimental results indicate that the release of the stored heat is more difficult. The amount of water taken up and the energy released by the material turned out to be strongly dependent on the water vapor pressure, temperature, and the total system pressure.

In this paper, we investigate the suitability of  $\text{MgSO}_4$  as a thermo-chemical storage material by using a finite volume method of analysis for its hydration reaction in a packed bed reactor. Effect of porosity of the packed bed, pressure drop across the reactor vessel, particle diameter of the salt, concentration of water vapor at inlet, and heat capacity of the reactor wall on thermal dynamics in terms of adsorption-desorption reaction and temperature profile at the outlet of the reactor with time are analyzed. We also investigate the effect of porosity of the reactor bed on outlet temperature experimentally..

## 2. MATHEMATICAL MODELLING

### Adsorption kinetics

The attraction between adsorbate molecules and adsorbent surface involve molecular forces otherwise known as Van Der Waal's forces. This physical adsorption is characterized by the liberation of heat [19]. In this study moist air at ambient temperature is modelled to flow through a porous bed of dry  $\text{MgSO}_4$ , the water vapour in the moist air absorbed by the dry  $\text{MgSO}_4$ , liberating heat to the surroundings. Thus the air at the outlet will be of higher temperature and lower relative humidity than the inlet condition. The problem domain is shown in Fig 1.

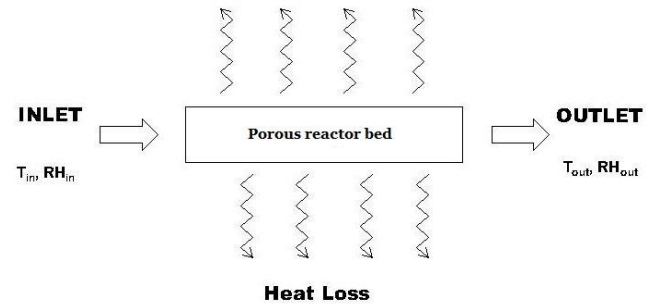
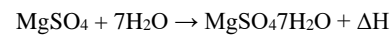


Fig.1 Simulated domain

The chemical reaction of this process is shown below.



Where  $\Delta H$  is the heat liberated during the reaction.

From the chemical reaction, it can be seen that one mole of  $\text{MgSO}_4$  adsorbs 7 moles of  $\text{H}_2\text{O}$  to form one mole of  $\text{MgSO}_4 \cdot 7\text{H}_2\text{O}$  and liberate 100 kJ of heat. Using this data, the maximum number of moles of  $\text{H}_2\text{O}$  that can be absorbed by 1 kg of  $\text{MgSO}_4$  is calculated. When the vapor comes in contact with the salt, the amount of vapor adsorbed, 'q' is always less than the maximum possible. It depends on the partial pressure of the water vapor and the temperature. The adsorption kinetics of the system is represented by the linear driving force (LDF) approximation

$$\frac{dq}{dt} = k_m(q_{eq} - q) \quad (1)$$

Where 'q' and 'q<sub>eq</sub>' are the originally absorbed and equilibrium mole of water by dry  $\text{MgSO}_4$  and 'k<sub>m</sub>' is the mass transfer coefficient.

The equilibrium loading of water on  $\text{MgSO}_4$  is estimated by Langmuir isotherm

$$q_{eq} = q_{max} \frac{bp}{1 + bp} \quad (2)$$

Where 'p' is the partial pressure of the vapour and 'b' is given by the following equation.

$$b = Ae^{(-\Delta H/RT)} \quad (3)$$

'A' is the Arrhenius factor for the chemical reaction, 'R' is the universal gas constant, T is the temperature, and 'ΔH' is the heat of adsorption.

The mass transfer coefficient 'k<sub>m</sub>' is given by

$$k_m = \left( \frac{d_p}{6k_f} + \frac{d_p^2}{60 \epsilon_b D_p} \right) \quad (4)$$

Where d<sub>p</sub> is the particle diameter, k<sub>f</sub> is the mass transfer coefficient for the fluid film around the particle, ε<sub>b</sub> is the porosity and D<sub>p</sub> is the macro pore diffusivity.

The process involving adsorption or evaporation the mass balance should include an axial dispersion term in terms of Sherwood number [21]. It was shown that the mass transfer coefficient could be expressed in terms of the dimensionless Sherwood number (Sh) by the relation

$$Sh = \frac{k_f D_p}{D_m} = 2 + 1.1Sc^{0.33}Re^{0.6} \quad (5)$$

Where 'Sc' is Schmidt number, Re is Reynold's number and D<sub>m</sub> is the molecular diffusivity. The macro pore diffusivity D<sub>p</sub> is a lumped parameter consisting of tortuosity factor (τ), molecular diffusivity (D<sub>m</sub>) and Knudsen diffusivity (D<sub>k</sub>).

In pores of diameter much greater than the mean free path of a molecule, diffusion occurs by a process of molecular collisions in the gas phase within the pore (called Maxwell or bulk diffusion), if the molecular mean free path is much greater than the pore diameter, diffusion occurs by molecules colliding with the pore walls (Knudsen diffusion).

$$D_p = \frac{1}{\tau} \left( \frac{1}{D_m} + \frac{1}{D_k} \right)^{-1} \quad (6)$$

### Assumptions

- The flow in the reactor can be described by an axially dispersed plug flow model.
- radial gradients in the bed are negligible; therefore, heat and mass transfer balances are considered as one-dimensional problems.
- the gas phase behaves as an ideal gas and is in thermal equilibrium with solid phase
- the adsorbent particles have identical characterizations and the bed properties are uniform.

Based on these assumptions, the governing heat and mass balance can be written by a set of partial differential equations with space coordinate z, and time coordinate t.

### Governing equations

Water mass balance equation

$$\frac{\partial c}{\partial t} + u \frac{\partial c}{\partial z} - D_z \frac{\partial^2 c}{\partial z^2} + \frac{(1 - \epsilon_b)}{\epsilon_b} \rho_p \frac{dq}{dt} = 0 \quad (7)$$

where, c is the water vapor concentration, ε<sub>b</sub> is the bed porosity, ρ<sub>p</sub> is the particle density of the salt, q is the average amount of adsorbed water per kg of salt, u is the velocity of flow and D<sub>z</sub> is the axial dispersion coefficient. This coefficient is derived from Wakao's relation,

$$\frac{\epsilon_b D_z}{D_m} = 20 + 0.5ReSc \quad (8)$$

where D<sub>m</sub> is the molecular diffusivity, Re is the Reynolds number ( $\frac{\rho_g \epsilon_b u d_p}{\mu_g}$ ), Sc is the Schmidt number ( $\frac{\mu_g}{\rho_g D_m}$ ) and μ<sub>g</sub> is the viscosity of the feed gas.

Energy balance

$$\begin{aligned} \rho C_p \frac{\partial T}{\partial t} + \epsilon_b \rho_g C_{p,g} u \frac{\partial T}{\partial z} - k_{eff} \frac{\partial^2 T}{\partial z^2} \\ - (1 - \epsilon_b) \rho_p \frac{dq}{dt} \Delta H \\ + \frac{4h_i}{d_i} (T - T_{wall}) = 0 \end{aligned} \quad (9)$$

In the above equation, T is the temperature of the gas, C<sub>p,g</sub> is the specific heat capacity of the gas, h<sub>i</sub> is the heat transfer coefficient of porous medium to the reactor wall, d<sub>i</sub> is the inner diameter of the reactor and T<sub>wall</sub> is the wall temperature.

The overall volumetric heat capacity ρC<sub>p</sub> is given by the following equation:

$$\begin{aligned} \rho C_p \\ = \epsilon_b \rho_g C_{p,g} + (1 - \epsilon_b) \rho_p C_{p,s} \\ + (1 - \epsilon_b) \rho_p q C_{p,water} M_{water} \end{aligned} \quad (10)$$

The overall volumetric heat capacity consists of the heat capacity of the air in bed voids, the heat capacity of the air in pores, the heat capacity of the solid and the heat capacity of the adsorbed water.

Here, C<sub>p,s</sub> is the specific heat capacity of the salt, C<sub>p,water</sub> is the specific heat capacity of water, and M<sub>water</sub> is the molar mass of the water.

The effective thermal conductivity, k<sub>eff</sub>, can be estimated using Zehner and Schlunder model.

$$\frac{k_{eff}}{k_g} = 1 - \sqrt{1 - \epsilon_b} \quad (11)$$

$$+ \frac{2\sqrt{1 - \epsilon_b}}{1 - \lambda B} \left( \frac{(1 - \lambda)B}{(1 - \lambda B)^2} \ln \frac{1}{\lambda B} - \left( \frac{B + 1}{2} \right) - \left( \frac{B - 1}{1 - \lambda B} \right) \right)$$

where,  $k_g$  is the thermal conductivity of the gas,  $\lambda = \frac{k_g}{k_p}$ ,  $k_p$  is the thermal conductivity of the salt, and the term B is the shape factor given by the following equation:

$$B = 1.25 \frac{(1 - \epsilon_b)^{10/9}}{\epsilon_b} \quad (12)$$

#### Reactor wall heat balance

In the above equation, the final term represents the heat loss from the packed bed to the reactor wall. It contains the term  $T_{wall}$  which is to be obtained from heat balance of the reactor wall.

$$A_{wall} \rho_{wall} C_{p,wall} \frac{\partial T_{wall}}{\partial t} \quad (13)$$

$$= \pi d_i h_i (T - T_{wall})$$

$$- \pi d_o h_o (T_{wall} - T_a)$$

where,  $A_{wall}$  is the cross sectional area of the wall,  $\rho_{wall}$  is the density of the wall,  $C_{p,wall}$  is the specific heat capacity of the wall,  $d_o$  is the outer diameter of the reactor vessel,  $h_o$  is the heat transfer coefficient of the wall to the atmosphere and  $T_a$  is the ambient temperature.

Heat is removed from the outer surface by natural convection and the value of the external heat transfer coefficient is obtained from the Nusselt number at the outside wall of the reactor [17].

$$Nu_o = \left( 2 + \frac{0.387 Ra^{1/6}}{(1 + (0.492/Pr)^{9/16})^{8/27}} \right)^2 \quad (14)$$

where,  $Ra$  is the Rayleigh number and  $Pr$  is the Prandtl number.

The heat transfer coefficient at the inside surface of a porous bed can be estimated using Leva's correlation [20].

#### Darcy's law

The governing equations described above require the velocity field. There are many empirical relations available for the velocity field in a porous medium. In this analysis Darcy's law is used.

Darcy's law relates the pressure drop (head) to the flow rate across a porous column. The velocity 'u' can be expressed as:

$$u = -\frac{K}{\mu} \Delta p \quad (15)$$

where,  $\Delta p$  is the pressure drop across the reactor and K is the permeability of the porous medium, where K is a function of porosity and particle diameter as given by the expression below:

$$K = \frac{\epsilon_b d_p^2}{180(1 - \epsilon_b)^2} \quad (16)$$

These governing equations are being non-dimensionalised and then discretized using finite volume method and solved. The reactor wall heat balance equation is discretized using FDM method since there is no requirement of spatial discretization.

The various parameters affecting the performance of the system are pressure drop across the reactor ( $\Delta p$ ), particle diameter of the salt ( $d_p$ ), water vapour concentration at inlet (c), porosity of the packed bed ( $\epsilon_b$ ), and thermal mass of the reactor wall ( $\rho_{wall} C_{p,wall}$ ).

#### Grid independence and validation

A grid independence study is performed to model the domain, Fig 2 shows the non dimensional temperature change as a function of non dimensional time at varying grid sizes at  $z = 0.5$ ,  $\epsilon_b = 0.7$ ,  $\Delta p = 0.4$ ,  $d_p = 35\text{mm}$ ,  $c = 0.6 \text{ mol/m}^3$  and  $\rho_{wall} C_{p,wall} = 10000$ . Where 'z' is the position (centre of the reactor).

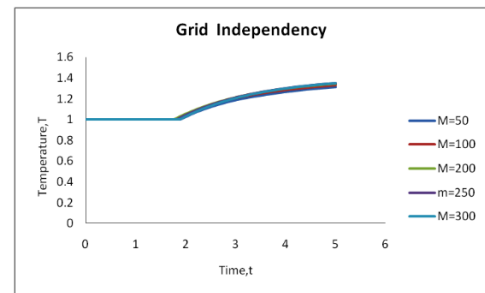


Fig 2. Grid Independence Test

The analysis is done for 5 different grid sizes with the number of grid points  $M = 50, 100, 200, 250,$  and  $300$ . It is evident from Fig 2 that the results become grid independent at  $M=250$ . The variation of temperature between grid point  $M=250$  and  $M=300$  is less than 1% (Table 1).

In order to validate the model, the results thus obtained were compared with the experimental data (shown in Fig 3) for hydration of Zeolite 13 X reported by Gaeini et al. [17]. Fig 3 shows the transient variation of temperature at different positions of the reactor.

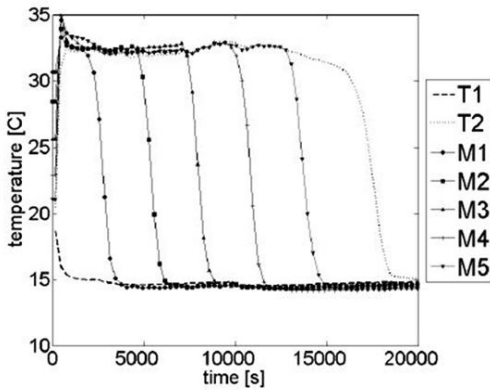


Fig 3(a). Temperature vs. time for different positions Gaeni et al. [17]

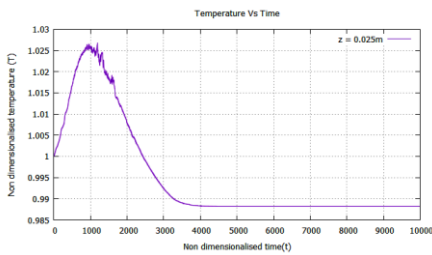


Fig 3(b). Non dimensional Temperature vs. Non dimensional time for validation

The reactor used in the work by Gaeni et al [17] was of 0.1 m length. M1 in Fig 3(a) represents the temperature at 0.025 m. It reaches to a value of almost 35 °C at a time of about 1000 s. This value is compared with the result (Fig 3(b)) obtained from the present model with the same working material and working conditions as in the case of Gaeni et al. Fig 4 shows the variation in non-dimensional temperature as a function of non-dimensional time, varying from time  $t=0$  to 10000. The non dimensional temperature reaches a maximum of 1.027 at about  $t=1000$ . The equivalent value of maximum temperature obtained by multiplying the reference value of temperature (300 K) is 308.1 K (35.1 °C) and the time is 1000 s. These results are same as the result from Gaeni et al [17], thereby the model is validated.

### 3. EXPERIMENTAL SETUP

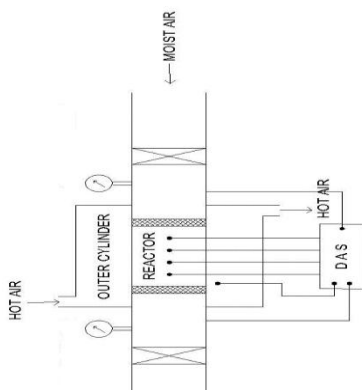


Fig. 4. Schematic model of Reactor

The fig. 4 shows the schematic of the experiment setup. It consists of a packed bed reactor surrounded by a stainless-steel cylinder for charging process. Electrically operated hot air gun is used to dehydrate (charge) the salt, it can be replaced by solar heating system. The inlet outlet and intermediate temperature readings are taken by six thermocouples placed inside the reactor and at inlet and outlet. The velocity of moist air is measured by an anemometer and pressure gauges are provided to find the pressure drop across the reactor. All the data are given to the data acquisition system (DAS) which consists of MAX 6675 amplifiers, ARDUINO board system and a computer. The entire setup is insulated to minimize the heat loss.

The salt material  $MgSO_4 \cdot 7H_2O$  is dehydrated by allowing hot air to flow around the reactor. The complete dehydration occurs about 175°C, so the temperature of hot air is set to be higher than this considering the heat loss to the surroundings and heat transfer loss in the reactor. In the experiment the temperature is set 200°C. The temperatures inside the reactor is observed, if it reaches about 175°C we can say that the whole salt material is dehydrated. Thermal energy is stored in the material during this charging or dehydration process.

To harvest the energy stored, moist air is passed through the reactor. The water molecules in the moist air reacts with the dehydrated salt and releases the energy in the form of heat, thereby increasing the outlet temperature of air. The rate of reaction mainly depends on the water content in the air, mass flow rate and porosity of the reactor bed.

## 4. RESULTS AND DISCUSSION

### Numerical analysis

The modeling of the domain is carried out with grid size 250 and with the following boundary conditions porosity = 0.75, pressure drop = 0.3 bar, particle diameter = 35  $\mu m$ , inlet water vapor concentration = 0.9 mol/m<sup>3</sup> and wall heat capacity = 26720 J/ m<sup>3</sup>K. The results of the modeling are presented in this section. Fig.5 shows the variation of temperature with time at various axial positions,  $z=0.25, 0.5, 0.75, 1$ .

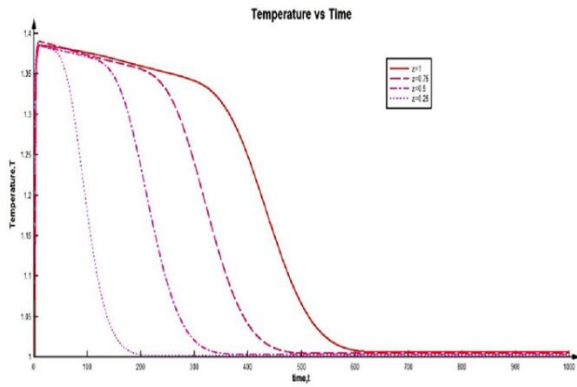


Fig 5. Axial distribution of Non-Dimensional Temperature

For  $z=1$ , the temperature remains at  $T=1$  up to  $t=0.255$ , then suddenly increases up to a maximum value of  $T=1.38$  following which it linearly decreases up to  $t=350$ . It then decreases suddenly up to  $t=550$  after which it decreases asymptotically and reach the initial value at  $t=624$ . The temperatures at other points also follow similar pattern. The rate of increase is maximum for  $z=0.25$  compared to the other positions. This happens because thermo-chemical reaction starts only when the water vapor is available at the inlet. Since the adsorption process is exothermic, the enthalpy of adsorption gets liberated as heat and during this process water vapor gets adsorbed. So, the salt particles nearer to the inlet get into contact with the water vapor early than the particles at locations away from the inlet. The temperature starts to decrease due to heat losses through the reactor wall to the surrounding. As the moist air entering from the inlet is at ambient temperature, it also absorbs heat and the overall temperature decreases.

As the moist air flows through the porous medium, the vapor is adsorbed by the salt particles. Therefore, the air at the exit of the reactor will be mostly dry. This is evident from vapor concentration  $c=0$  up to  $t=10$  at the outlet (Fig 6). After  $t=10$ , the vapor concentration increases and reaches the value equal to the inlet condition and remains constant at that value. This is because the adsorption process is completed all along the reactor, and no more vapor adsorption is possible in the reactor.

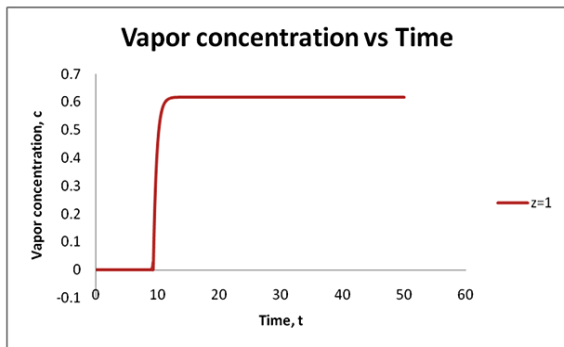


Fig 6. Non-Dimensional Vapor concentration vs. Non-Dimensional time at outlet

According to the Orthogonal Array described earlier, 16 different simulations were conducted up to time  $t=1000$ . Three different responses were recorded. The three different time responses are:

- Beginning of the temperature rise of the air at the outlet of the reactor.
- Air temperature attaining at the outlet, and
- Heat carried away by the air at the outlet.

$$Q = \rho_g C_{p,g} \frac{\pi d_i^2}{4} u \int \Delta T dt$$

This can be obtained from the integration of the  $\Delta T$  vs t curve

*Effect of porosity*

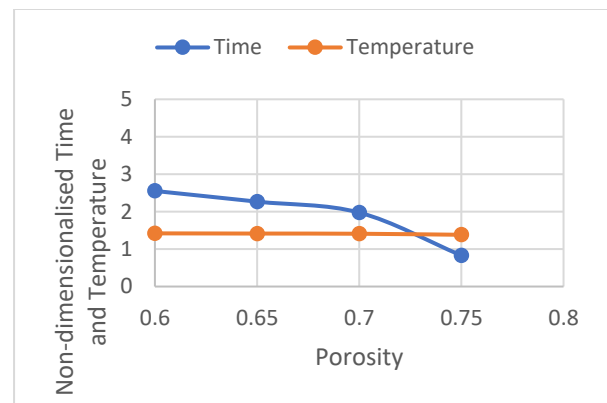


Fig 7. Non-dimensional time, Max Non-Dimensional Temperature as a function of porosity, Thaguchi method

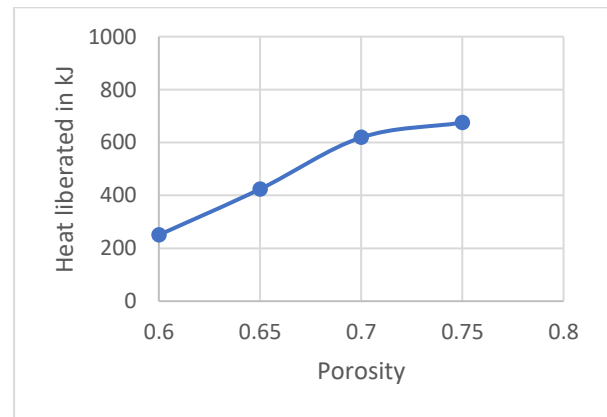


Fig. 8. Heat liberated as a function of porosity, Thaguchi method

Porosity is the ratio of the void space to the total space in the domain. More porous the medium, lesser the amount of salt in the domain and faster the flow of moist air through the medium. Fig.7 shows the effect of porosity on time required to start the reaction the effect of porosity on the

maximum temperature attained at the outlet. The total heat liberated during the process is shown in Fig.8. It can be seen that as the porosity increases the time required to attain temperature rise decreases. This is due to the fact that the velocity of flow is higher when the porosity is high, which leads to a faster rate of adsorption and heat release. The maximum temperature attained at the outlet of the domain decreases as the porosity increases. This can be attributed to the higher velocity of flow, leading to lower residence time. But the heat liberated during the time interval  $t=0$  to  $t=1000$  in the form of sensible heating of the outlet air, increases with the porosity.

**Experimental analysis**

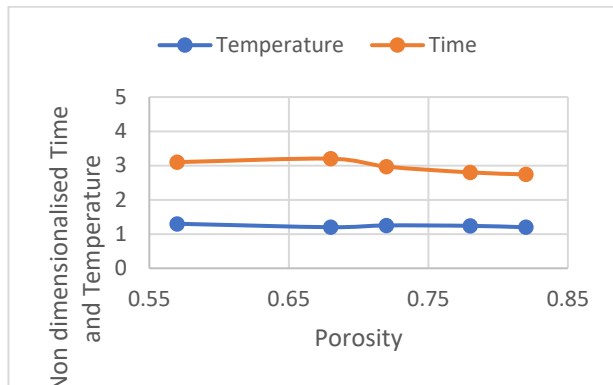


Fig. 9. Non-dimensionalised Time and Temperature (from experiment)

Figure 9 shows the result from experimental analysis of the thermochemical reactor, the maximum temperature at the reactor outlet in all the trials are lesser than the value obtained in numerical analysis and the time required to initiate the reaction is more. The residence time plays an important role in the reaction and time to start the reaction, if residence time is less (moist air with high velocity) it will take more time to start the reaction inside the reactor, the temperature rise will also be affected by the less residence time.

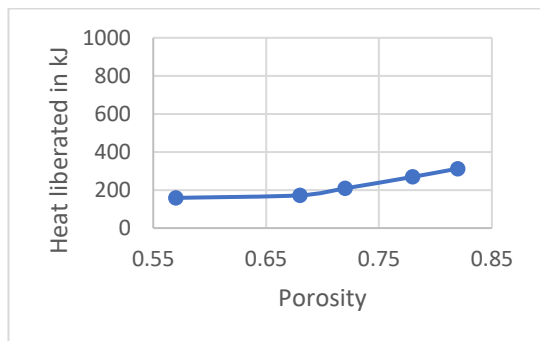


Fig. 10. Heat liberated (from experiment)

Figure 10. shows the heat liberated from the reactor bed, the heat liberated is the area under the  $\Delta T$  Vs.  $t$  curve. The results show the same trend of the numerical analysis but the values

obtained from the experimental analysis is much lower than that of numerical analysis. The heat loss through the walls of the reactor could be a major reason for this. In experimental setup the wall of the reactor is not insulated because dehydration is taking place by applying heat at the walls of the reactor. At lower void fractions the heat liberated is less because of less salt material (more void space), and if porosity is lesser the heat liberated is higher due to the large amount of salt material.

**5. CONCLUSION**

Modeling of energy release from a fixed bed filled with  $MgSO_4$  on hydration using the finite volume method shows the effect various design and operating parameters on the performance of the bed. The porosity of the bed plays an important role in determining the velocity of flow in the medium along with the pressure drop. Since the void space between the particles increases with porosity, the temperature of the outlet air increases at a higher rate. But the maximum temperature attained for the same flow rate is found to decrease when both porosity and pressure drop increase, because of less residence time of the air and less amount of thermochemical material. The particle diameter plays an important role on adsorption kinetics. Finer the particle size, larger is the mass transfer coefficient. Another important factor which affect the performance of the reactor is the vapor concentration of the inlet air. Higher the vapor concentration of supply moist air, faster is the reaction rate and lesser the time required to attain the maximum temperature. Thus, while designing a thermochemical reactor, the porosity of the reactor, mass flow rate of moist air, particle diameter of the salt, and vapor concentration of the inlet moist air are to be optimized to get the maximum performance from the reactor bed

The experiment focuses on the performance analysis of a thermochemical reactor with varying porosities and the effect of porosity on the key factors like time to initiate the reaction, Maximum temperature attained and heat liberated in the discharging process.in the energy release. The results show a good agreement with the numerical prediction. The heat liberated during the hydration process is less than the numerical prediction and the reason is that the loss of heat through the reactor wall. This can be eliminated by removing the outer cylinder for heating the thermochemical material. The charging process can be done by allowing hot dry nitrogen gas to flow through the reactor bed. This will vapourise the water content in the salt and take away with the gas.

Another important thing is the suitability of  $MgSO_4$  as an energy storage material with high energy density. From this study it is shown that  $MgSO_4$  is a promising candidate in low to medium temperature energy storage and the system can be easily integrated with solar collectors for charging process.

**6. FUTURE SCOPE**

This work can be extended to check the suitability of new composite materials for better performance as storage medium in thermochemical energy storage for both low and high temperature applications. In this work we analysed the effect of porosity of the reactor bed only, but several other parameters like particle diameter, pressure drop across the bed, water vapour flow rate etc. are also have significant effect on the performance of the storage system. A thorough understanding in the effect

of these parameters would help the researchers to design a more efficient storage system.

The problem associated with experimental analysis of thermochemical energy storage system are need more researches especially in the area of heat transfer mechanism, reaction kinetics, controlled release of stored energy etc.

**Conflict of Interest:** No conflict of interests

## REFERENCES

- [1]. Juan Wu, and Xin feng Long, Research progress of solar thermochemical energy storage, International Journal Of Energy Research. (2014) DOI: 10.1002/er.3259
- [2]. Omar Al-Abbasi, Abdessattar Abdelkefi and Mehdi Ghommem, Modeling and assessment of a thermochemical energy storage using salt hydrates, International Journal Of Energy Research (2017), DOI: 10.1002/er.3776
- [3]. J. Cot-Gores, A. Castell, L.F. Cabeza, Thermochemical energy storage and conversion: A-state-of-the-art review of the experimental research under practical conditions, Renew. Sust. Energ. Rev. 16 (2012) 5207-5224. DOI: 10.1016/j.rser.2012.04.007.
- [4]. K. Darkwa, P.W. O'Callaghan, Green transport technology (GTT): Analytical studies of a thermochemical store for minimising energy consumption and air pollution from automobile engines, Appl. Therm. Eng. 17 (1997) 603-614. DOI: 10.1016/S1359-4311(97)80001-4.
- [5]. H. Druck, B. Mente, H. Kerskes, Concepts of long term thermochemical energy storage for solar thermal applications- selected examples, Energy Procedia. 30 (2012) 321-330. DOI: 10.1016/j.egypro.2012.11.038
- [6]. A. Solé, X. Fontanet, C. Barreneche, A.I. Fernández, I. Martorell, L.F. Cabeza, Requirements to consider when choosing a thermochemical material for solar energy storage, Solar Energy. 97 (2013) 398-404.
- [7]. D. Aydin, S.P. Casey, S. Riffat, The latest advancements on thermochemical heat storage systems, Renew. Sust. Energ. Rev. 41 (2015) 356-367. DOI: 10.1016/j.rser.2014.08.054.
- [8]. A. Agarwal, R.M. Sarviya, An experimental investigation of shell and tube latent heat storage for solar dryer using paraffin wax as heat storage material, JESTECH. 19 (2016) 619-631. DOI: 10.1016/j.jestech.2015.09.014.
- [9]. Y.I. Aristov, D.M. Chalaev, B. Dawoud, L.I. Heifets, O.S. Popel, G. Restuccia, Simulation and design of a solar driven thermochemical refrigerator using new chemisorbents, Chem. Eng. J. 134 (2007) 58-65. DOI: 10.1016/j.cej.2007.03.070.
- [10]. G. Balasubramanian, M. Ghommem, M.R. Hajj, W.P. Wong, J.A. Tomlin, I.K. Puri, Modeling of thermochemical energy storage by salt hydrates, Int. J. Heat Mass Transf. 53 (2010) 5700-5706. DOI: 10.1016/j.ijheatmasstransfer.2010.08.012.
- [11]. M. Ghommem, G. Balasubramanian, M.R. Hajj, W.P. Wong, J.A. Tomlin, I.K. Puri, Release of stored thermo- chemical energy from dehydrated salt, Int. J. Heat Mass Transf. 54 (2011) 4856-4863. DOI: 10.1016/j.ijheatmasstransfer.2011.06.041.
- [12]. M.N. Azpiazu, J.M. Morquillas, A. Vazquez, Heat recovery from a thermal energy storage based on the Ca(OH)<sub>2</sub>/CaO cycle, Appl. Therm. Eng. 23 (2003) 733-741. DOI:10.1016/S1359-4311(03)00015-2.
- [13]. F. Bertsch, B. Mente, S. Asenbeck, H. Kerskes, H. Müller-Steinhagen, Low temperature chemical heat storage - an investigation of hydration reactions. Technical report, Institute for Technical Thermodynamics, German Aerospace Centre. (2009).
- [14]. H.A. Zondag, M. Van essen, L.P.J. Bleijendaal, B. Kikkert, M. Bakker. Application of MgCl<sub>2</sub>·6H<sub>2</sub>O for thermochemical seasonal solar heat storage, 5th International Renewable Energy Storage Conference, 2010.
- [15]. A.H. Abedin, M.A. Rosen, Assessment of a closed thermochemical energy storage using energy and exergy methods, Appl. Energy. 93 (2012) 18-23. DOI: 10.1016/j.apenergy.2011.05.041.
- [16]. D. Stitou, N. Mazet, S. Mauran, Experimental investigation of a solid/gas thermochemical storage process for solar air-conditioning, Energy. 41 (2012) 261-270. DOI: 10.1016/j.energy.2011.07.029.
- [17]. V.M. van Essen, H.A. Zondag, J. Cot Gores, L.P.J. Bleijendaal, M. Bakker, R. Schuitema, W. van Helden, Z. He, C.C.M. Rindt, Characterization of MgSO<sub>4</sub> Hydrate for Thermochemical Seasonal Heat Storage, J. Sol. Energy Eng. 131(2009), 041014. DOI:10.1115/1.4000275.
- [18]. M.Gaeini, H.A. Zondag, C.C.M. Rindt, Non-isothermal kinetics of zeolite water vapor adsorption into a packed bed lab scale thermochemical reactor, International Heat Transfer Conference, 2014. Proceedings of the IHTC-15, IHTC15-9169-1/11.
- [19]. D.C. Montgomery, Design and Analysis of Experiments, eighth ed., Wiley, United States, 2013.